CONF-8910222--9

CAST STAINLESS STEEL AGING: MECHANISMS AND PREDICTIONS*

O. K. Chopra and H. M. Chung

Materials and Components Technology Division
ARGONNE NATIONAL LABORATORY
9700 South Cass Avenue
Argonne, Illinois 60439 U.S.A.

CONF-8910222--9

DE90 003772

October 1989

Presented at the 17th Water Reactor Safety Information Meeting, Rockville, MD., October 23-25,1989.

*Work supported by the Office of Nuclear Regulatory Research, U. S. Nuclear Regulatory Commission.

CAST STAINLESS STEEL AGING: MECHANISMS AND PREDICTIONS*

O. K. Chopra and H. M. Chung

Materials and Components Technology Division, Argonne National Laboratory,
9700 South Cass Avenue, Argonne, IL 60439, U.S.A.

Abstract

Charpy-impact and J-R curve data are presented for several experimental and commercial heats, as well as for reactor-aged material of CF-3, CF-8, and CF-8M grades of cast stainless steel. The effects of material variables on the embrittlement of cast stainless steels are evaluated. In general, the low-carbon CF-3 grades of cast stainless steels are the most resistant and molybdenum-containing high-carbon CF-8M grades are the most susceptible to low-temperature embrittlement. The ferrite morphology has a strong effect on the extent or degree of embrittlement, while material composition influences the kinetics of embrittlement. The kinetics of embrittlement can vary significantly with small changes in the constituent elements of the cast material. The mechanisms of embrittlement have also been established. Mechanical property data have been analyzed to develop the procedure and correlations for predicting the kinetics and extent of embrittlement of reactor components from known material parameters. The method and examples of estimating the impact strength and fracture toughness of cast components during reactor service are described. The lower–bound values of impact strength and fracture toughness for cast stainless steels at LWR operating temperatures are defined.

1. Introduction

A program is being conducted to investigate the significance of low-temperature embrittlement of cast duplex stainless steels under LWR operating conditions and to evaluate possible remedies to the embrittlement problem for existing and future plants. The scope of the investigation includes the following goals: (1) establish the aging mechanism and validate the simulation of in–reactor degradation by accelerated aging, (2) establish the effects of key compositional and metallurgical variables on the kinetics and extent of embrittlement, and (3) obtain fracture toughness data on long–term–aged materials for extrapolation to predict the degree of toughness loss suffered by cast stainless steel components during normal and extended service life of reactors.

Microstructural and mechanical properties data are being obtained on 19 experimental heats (static-cast keel blocks) and six commercial heats (centrifugally cast pipes and a static-cast pump impeller and pump casing ring) as well as reactor-aged material of CF-3, CF-8, and CF-8M grades of cast stainless steel. Six of the experimental heats are also in the form of 76-

---

* RSR FIN Budget No. A2243; RSR Contact: J. Muscara.

mm-thick slabs. The reactor-aged material is from the recirculating cover plate assembly of the KRB reactor, which was in service in Gundremmingen, FRG, for ~12 yrs (~8 yr at service temperature of 284°C). Fractured impact test bars from five heats of aged cast stainless steel were obtained from Georg Fischer Co. (GF), Switzerland, for microstructural characterization. The materials are from a previous study of long-term aging behavior of cast stainless steel.[1] The data on chemical composition, ferrite content, hardness, ferrite morphology, and grain structure of the experimental and commercial heats have been reported elsewhere.[2-6] The ferrite content of the cast materials ranges from 3 to 30%. The chemical composition, hardness, and ferrite content and distribution of some of the cast materials are given in Table 1. Specimen blanks for Charpy-impact, tensile, and J-R curve tests are being aged at 290, 320, 350, 400, and 450°C for times up to 50,000 h.

The mechanical property data for several heats of cast stainless steel aged up to 30,000 h have been presented earlier.[7-9] A preliminary assessment of the processes and significance of the thermal aging in cast stainless steels was also presented.[9] The results indicate that thermal aging at temperatures below 500°C increases the tensile strength and decreases the impact energy and fracture toughness of the steels. The Charpy transition curve shifts to higher temperatures. Different heats exhibit different degrees of embrittlement. For all grades of cast stainless steel, the extent of embrittlement increases with an increase in ferrite content. The low-carbon CF-3 grades are the most resistant, and the molybdenum-containing high-carbon CF-8M grades are least resistant to embrittlement.

Embrittlement of cast stainless steels results in a brittle fracture associated with either cleavage of the ferrite or separation of the ferrite austenite phase boundary. The latter generally occurs in the high-carbon grades because of the presence of large $M_{23}C_6$ carbides at the phase boundaries. For CF-8 steels, the phase boundary carbides form during the production heat treatment of the casting. Consequently, the unaged CF-8 steels exhibit low lower-shelf energy and high mid-shelf Charpy transition temperature (CTT) relative to the CF-3 steels. The fracture mode for CF-8 steels in the lower-shelf or transition temperature regime is predominantly phase boundary separation, Fig. 1.[7,8] In contrast, the CF-3 grades show a dimpled ductile failure. Fracture by phase boundary separation is observed in only a few heats of unaged CF-8M grades, depending on whether or not the material contains phase boundary carbides. The metallographic data indicate that additional precipitation of phase boundary carbides and/or growth of existing carbides occurs in the high-carbon steels during thermal aging, particularly after aging at 400 or 450°C.[8]

The mechanical property data also indicate that the kinetics and extent of embrittlement are controlled by several mechanisms that depend on material parameters as well as aging temperature. Materials aged at 450°C show significant precipitation of phase boundary carbides (also nitrides in high-nitrogen steels) and a large decrease in ferrite content of the material.[9] Furthermore, the decrease in ferrite is significantly greater for CF-8M steels than for the other grades. Such processes either do not occur or their kinetics are extremely slow at reactor temperatures. Consequently, data obtained at 450°C aging are not representative of

Table 1. Product Form, Chemical Analysis, Hardness, and Ferrite Morphology of Various Heats of Cast Stainless Steel

Heat	Grade	Product Form	Size (mm)	Composition (wt %)							Hardness	Ferrite Content (%)		Ferrite Intercept (μm)
				C	N	Mn	Si	Ni	Cr	Mo	R_B	Calc.	Meas.	
56	CF-8	Keel B.	180 x 120 x 30-90	0.066	0.030	0.57	1.05	9.28	19.65	0.34	82.5	7.3	10.1	84
59	CF-8			0.062	0.045	0.60	1.08	9.34	20.33	0.32	83.2	8.8	13.5	75
61	CF-8			0.054	0.080	0.65	1.01	8.86	20.65	0.32	85.2	10.0	13.1	82
60	CF-8			0.064	0.058	0.67	0.95	8.34	21.05	0.31	86.7	15.1	21.1	63
47	CF-3			0.018	0.028	0.60	1.06	10.63	19.81	0.59	79.6	8.4	16.3	68
52	CF-3			0.009	0.052	0.57	0.92	9.40	19.49	0.35	81.6	10.3	13.5	69
51	CF-3			0.010	0.058	0.63	0.86	9.06	20.13	0.32	83.8	14.2	18.0	52
63	CF-8M			0.055	0.031	0.61	0.58	11.85	19.37	2.57	81.5	6.4	10.4	81
65	CF-8M			0.049	0.064	0.50	0.48	9.63	20.78	2.57	89.9	20.9	23.4	43
64	CF-8M			0.038	0.038	0.60	0.63	9.40	20.76	2.46	89.7	28.9	28.4	41
P1	CF-8	Pipe	890 OD 63 wall	0.036	0.056	0.59	1.12	8.10	20.49	0.04	84.9	17.7	24.1	90
P2	CF-3	Pipe	930 OD 73 wall	0.019	0.040	0.74	0.94	9.38	20.20	0.16	83.8	12.4	15.6	69
I	CF-3	Impeller	NA	0.019	0.032	0.47	0.83	8.65	20.14	0.45	81.0	20.9	17.1	65
P4	CF-8M	Pipe	580 OD 32 wall	0.040	0.151	1.07	1.02	10.00	19.64	2.05	83.1	5.9	10.4	182
68	CF-8	Slab	610 x 610 x 76	0.063	0.062	0.64	1.07	8.08	20.64	0.31	84.6	14.9	23.4	87
69	CF-3	Slab	610 x 610 x 76	0.023	0.028	0.63	1.13	8.59	20.18	0.34	83.7	21.0	23.6	35
74	CF-8M	Slab	610 x 610 x 76	0.064	0.048	0.54	0.73	9.03	19.11	2.51	85.8	15.5	18.4	90
75	CF-8M	Slab	610 x 610 x 76	0.065	0.052	0.53	0.67	9.12	20.86	2.58	89.5	24.8	27.8	73
KRB	CF-8	Pump Cover Plate		0.062	0.038	0.31	1.17	8.03	21.99	0.17	–	27.7	34.0	173

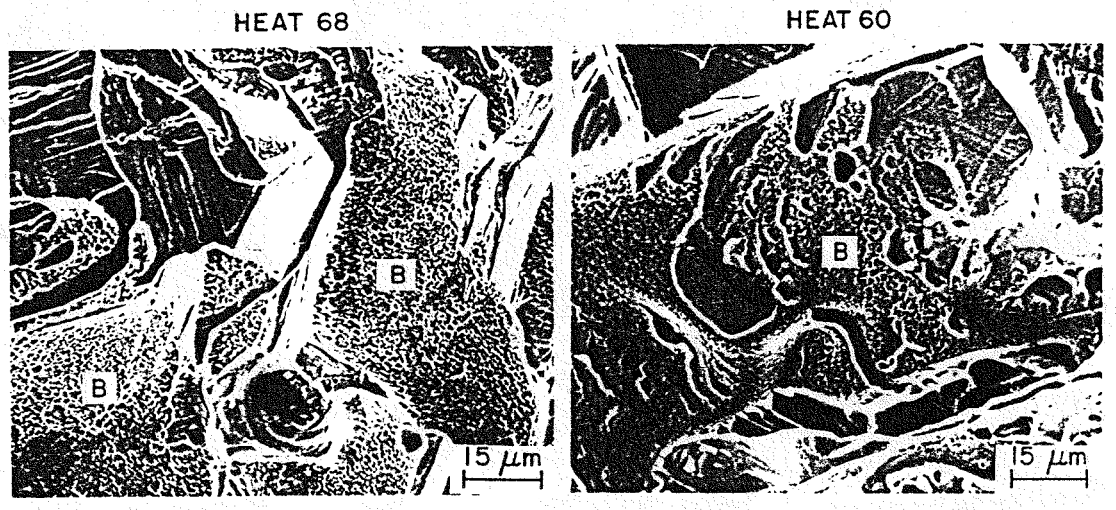

Figure 1. Fracture Surface of Charpy-Impact Specimens of Unaged CF-8 Steel Tested at -196°C. Fracture mode B = phase boundary separation.

reactor operating conditions and extrapolation of the 450°C data to predict the extent of embrittlement at reactor temperatures is not valid.

This paper presents a summary of the mechanical property data for several heats of cast stainless steel aged up to 30,000 h at 290, 320, 350, and 400°C. The results are analyzed to develop the procedure and correlations for predicting the kinetics and extent of embrittlement of reactor components from known material parameters. The mechanisms of thermal embrittlement of cast stainless steels are also discussed.

2. Room Temperature Impact Energy

The results from room-temperature Charpy-impact tests on the various experimental and commercial heats, aged up to 30,000 h at 290, 320, 350, and 400°C, were analyzed to determine the kinetics and extent of embrittlement. The variation of the Charpy-impact energy (KCV) with time can be expressed as

$$KCV = K_m + \beta\{1 - \tanh [(P - \theta)/\alpha]\}, \quad (1)$$

where P is the aging parameter, K_m is the minimum impact energy reached after long-term aging, β is half the maximum decrease in impact energy, θ is the log of the time to achieve β reduction in impact energy, and α is a shape factor. The aging parameter represents the time to achieve a specific degree of aging at 400°C. The aging time to reach a given degree of embrittlement at different temperatures is determined from the equation

$$t = 10^P \exp\left[\frac{Q}{R}\left(\frac{1}{T} - \frac{1}{673}\right)\right] \quad (2)$$

where Q is the activation energy, R the gas constant, T the absolute temperature, and P the aging parameter that represents the degree of aging reached after 10^P h at 400°C.

The values of the constants in Eqs. (1) and (2) were obtained from the best fit of the Charpy data for various heats of cast stainless steel aged up to 30,000 h at 290, 320, 350, and 400°C. The activation energies, with the 95% confidence limits, are given in Table 2. The Charpy impact data for three of the heats are plotted as a function of aging time in Fig. 2, along with the fitted curves of the form given by Eqs. (1) and (2). The confidence limits are large for some heats because of the relatively small decrease in impact energy and significant scatter in the data. The Charpy data obtained from 290°C aging showed no reduction in impact energy even after aging for 30,000 h, rather, a slight increase in impact energy was observed relative to the unaged values. This increase in impact energy is real and was observed for most heats aged at low temperatures, i.e., 30,000 h at 290°C or 3,000 to 10,000 h at 320°C. The low-temperature aging data tends to bias the analyses to yield higher values of activation energies and, therefore, the 290°C aging results were excluded from the analysis to obtain the activation energies for some of the heats. Long-term aging data are needed to establish the kinetics of embrittlement between 320 and 290°C.

Table 2 Activation Energies for the Kinetics of Embrittlement for Various Heats of Cast Stainless Steels.

Heat	Ferrite, %		Material Parameter	Activation Energy , kJ/mole (kcal/mole)		
	Meas.	Calc.[a]	Φ[b]	Average	95% Confidence Limit	From Ref. 9
47	16.3	8.4	11.3	134 (32.1)	53-216 (12.6-51.6)[c]	92 (21.9)
51	18.0	14.3	11.9	218 (52.1)	116-320 (27.7-76.5)[c]	184 (44.1)
69	23.6	21.0	14.4	170 (40.6)	113-226 (27.0-54.1)[c]	-
56	10.1	7.3	14.1	-	-	234 (56.0)
59	13.5	8.8	23.8	-	-	196 (46.9)
60	21.1	15.4	54.6	240 (57.3)	194-285 (46.4-68.2)	199 (47.5)
68	23.4	14.9	92.1	166 (39.6)	133-199 (31.7-47.6)	-
P1	24.1	17.7	66.1	239 (57.1)	203-274 (48.5-65.6)	-
63	10.4	6.4	13.3	-	-	102 (24.3)
64	28.4	29.0	42.0	141 (33.8)	111-172 (26.5-41.0)	143 (34.1)
65	23.4	20.9	41.9	177 (42.2)	140-214 (33.4-51.1)	152 (36.4)
66	19.8	19.6	21.0	171 (40.9)	96-246 (23.0-58.7)[c]	126 (30.2)
75	27.8	24.8	116.7	159 (38.0)	138-180 (32.9-43.0)	-
P4	10.0	5.9	41.5	152 (36.3)	123-181 (29.5-43.2)	-

[a] Calculated from chemical composition with Hull's equivalent factor.

[b] $\Phi = \delta_m^2(C+0.4N)(Cr+Mo+Si)l/1000$ where δ_m is the measured ferrite content in %, l is the mean ferrite spacing in μm, and the concentrations of C, N, Cr, Mo, and Si in the cast stainless steel are in wt.%.

[c] Standard deviation is large because of the relatively small decrease in impact energy and large scatter in the data.

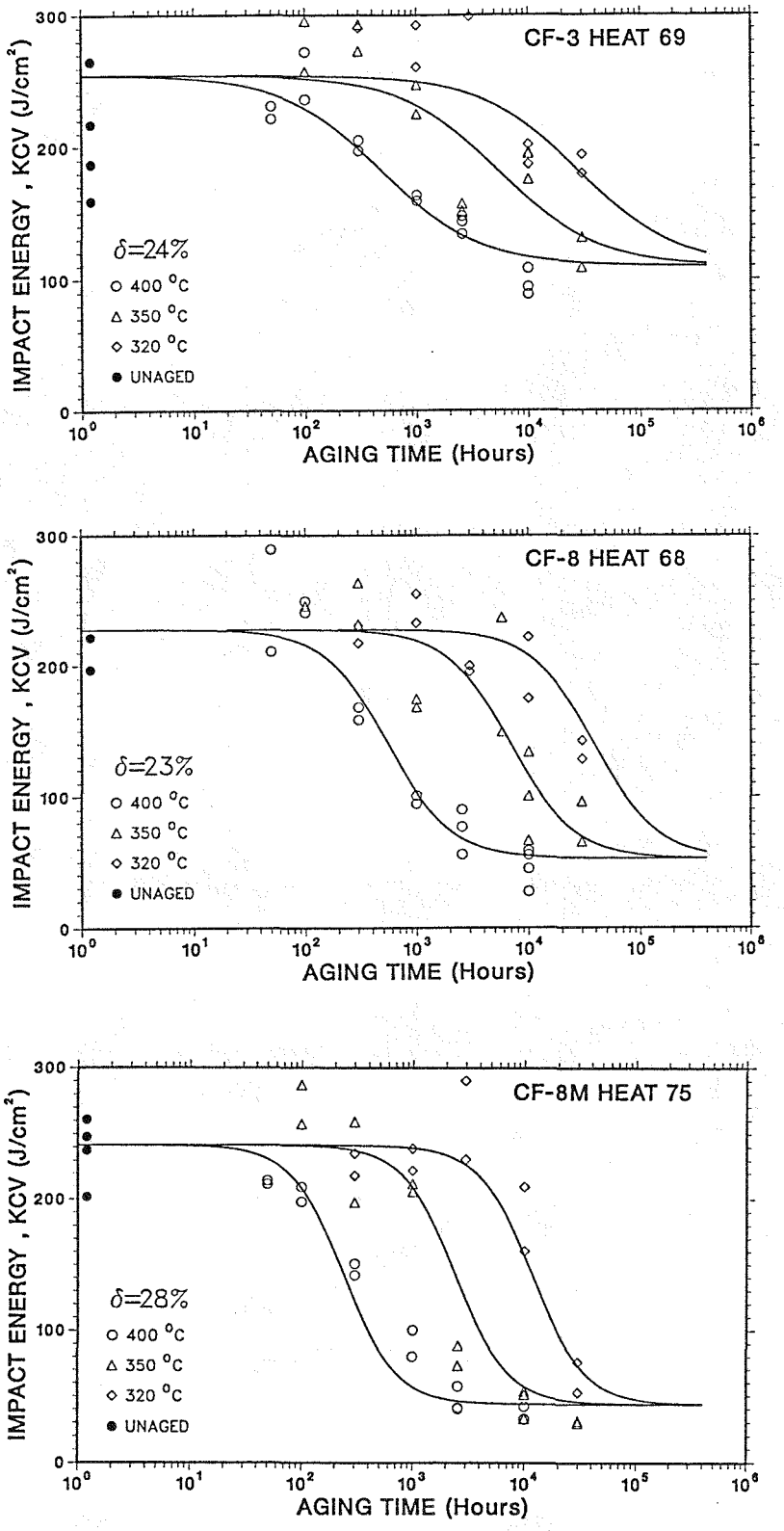

Figure 2. Effect of Thermal Aging on Room-Temperature Impact Energy of CF-3, CF-8, and CF-8M Cast Stainless Steel.

The activation energies reported earlier in Ref. 9 are also listed in Table 2. Charpy data for long-term aging (i.e., 30,000 h) at 320 and 290°C were not included in the analyses of Ref. 9. Thus, the calculated activation energies primarily represent the kinetics of embrittlement at temperatures between 400 and 350°C. These values are 15 to 20% lower than those determined from aging data at temperatures between 400 and 320°C. The results suggest that the activation energy for embrittlement is not constant in the temperature range of 400 and 290°C, but increases with a decrease in temperature. A similar behavior has been reported for several heats of CF-8M steels aged at temperatures between 400 and 300°C.[10] Consequently, the extrapolation of the 400°C aging data to reactor temperatures may not be valid and would yield conservative estimates of embrittlement for some of the heats of cast stainless steel.

3. Extent of Embrittlement

The Charpy-impact data obtained at room temperature were analyzed to develop a correlation between material variables and the extent or degree of embrittlement, i.e., minimum room-temperature impact energy [K_m in Eq. (1)] that would ever be achieved after long-term aging. It is well established that the extent of embrittlement increases with an increase in the ferrite content of the cast stainless steel. Furthermore, Charpy impact data for several heats of CF-8 and CF-8M steels aged for 10,000 h at 350 or 400°C, indicate that the impact energy decreases with an increase in the Cr content, irrespective of the ferrite content in the steel.[10] A better correlation was obtained when the total concentration of ferrite formers (i.e., Cr, Mo, and Si) are considered.[10] A sharp decrease in impact energy occurs when either the Cr content exceeds 18 wt.% or the concentration of Cr+Mo+Si exceeds 23.5 wt.%. The concentrations of C and N in the steel also increase the extent of embrittlement because of the contribution to phase boundary carbides or nitrides and the subsequent fracture by phase boundary separation. Consequently the data on the minimum room-temperature impact energy were analyzed using a exponential function of the various material variables. Best fit of the data were obtained with a material parameter Φ given by

$$\Phi = \delta_m^2 \, (C+0.4N) \, (Cr+Mo+Si) \, l \, (\times 10^{-3}), \qquad (3)$$

where the measured ferrite content δ_m is in %, the Cr, Mo, Si, C, and N contents are in wt.%, and the mean ferrite spacing l is in μm. The results indicate that both the amount and spacing of ferrite influence the extent of embrittlement. A similar correlation, but without the effect of ferrite spacing, has been proposed earlier by investigators at Electricité de France (EdF).*

The minimum impact energy is plotted in Fig. 3 as a function of the material parameter Φ. Results from the studies at Framatome (FRA),[11,12] Central Electricity Generating Board (CEGB),[13] and Electric Power Research Institute (EPRI)[14] are also shown in the figure. The data show a good correlation with the material parameter. The impact energy for the Framatome Heat 4331 (Ref. 12), however, is significantly lower than that predicted from Fig. 3. This heat contains 0.2% Nb. The fracture surface of the impact test specimens, Fig. 4, show that the phase boundaries are decorated with very large Nb carbides which crack easily. The

---

* M. Guttmann, EdF, private communications, October 1987.

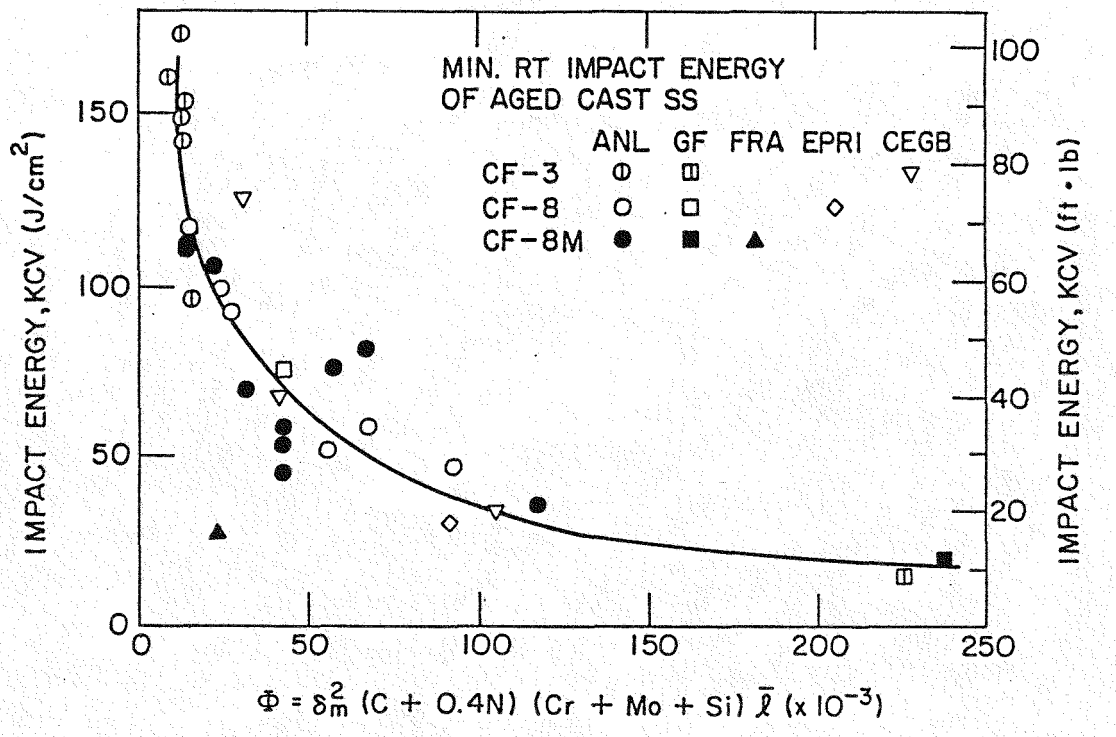

Figure 3. Correlation between Minimum Room Temperature Impact Energy and Material Parameter for Aged Cast Stainless Steel.

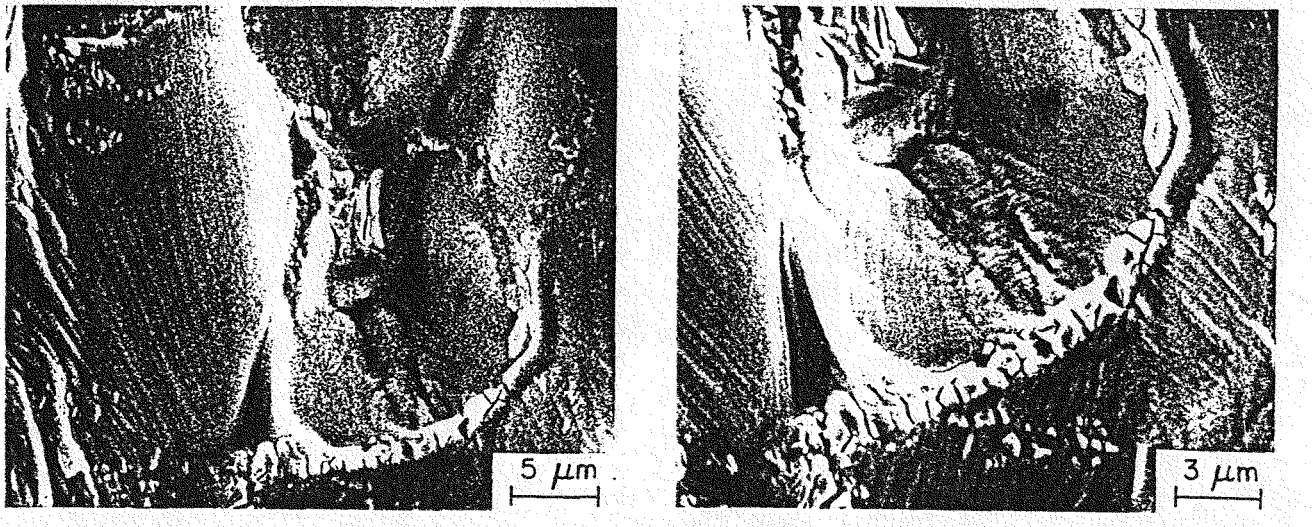

Figure 4. Fracture Surface of Charpy-Impact Specimen of Framatome Heat 4331 Aged for 700 h at 400°C and Tested at Room Temperature.

presence of large phase boundary carbides alters the deformation and fracture behavior of the material, i.e., initiation of cleavage by carbide cracking. A difference in the mode of fracture is reflected in the values of the yield and maximum loads for the instrumented Charpy tests, shown in Fig. 5 for the Framatome Heat 4331 and ANL Heat 74. The corresponding Charpy transition curves are shown in Fig. 6. Both heats are CF-8M grade and contain ~20% ferrite, yet the transition curves are significantly different. The 65-J (~50 ft·lb) transition temperature is 220°C for Heat 4331 aged for 700 h at 400°C and is 20°C for Heat 74 aged for 10,000 h at 400°C. The yield loads are comparable for both heats indicating similar degree of strengthening in the two heats. However, Fig. 5 shows that failure occurs at ~14 kN load in Heat 4331 and at ~18 kN load in Heat 74. The difference in the maximum load at failure suggests a difference in the fracture mechanism. The present correlation does not consider the effects of Nb on embrittlement.

The correlation in Fig. 3 indicates that the impact energy will be less than 50 J/cm^2 (30 ft·lb) for those cast stainless steels for which the material parameter is greater than ~60. For cast stainless steels containing >10% ferrite, the mean ferrite spacing is in the range of 40 to 200 μm; Cr + Mo + Si concentration is ~22% for CF-8 or CF-3 and ~24% for CF-8M; and N content is typically 0.04%. Thus, for cast materials with 0.06% C and 100 μm ferrite spacing, the impact energy will be below 50 J/cm^2 when the ferrite content is above 20%. However, cast materials with 10 or 15% ferrite can also reach very low impact strength when ferrite spacing or N content is high.

Figure 3 can be used to estimate the extent of embrittlement (expressed as room-temperature impact energy) for a specific cast stainless steel component. The variables in the material parameter can be determined nondestructively. The compositions are generally known, ferrite content can be calculated from the composition or measured with a ferrite scope. Ferrite spacing is the variable that is least readily available, but it can be determined by surface replica techniques. However, a conservative estimate of the possible extent of embrittlement can be obtained by assuming the highest value observed in the material data base, i.e., ferrite spacing of ~180 μm.

The significance of material parameter Φ on the extent of embrittlement is seen clearly in Fig. 7. The impact energies for several heats with comparable values of Φ are plotted as a function of the aging parameter P. The different temperatures and times of aging are normalized in terms of P by Eq. (2). The results show that the extent of embrittlement increases with an increase in Φ. For each range of Φ there is a saturation value of minimum impact energy. This behavior is independent of the kinetics of embrittlement, e.g., the extent of embrittlement is comparable for Heats 60, P1, 64, 65, and P4, while the activation energies range between 140 and 240 kJ/mole (34 and 57 kcal/mole). The ferrite content also varies significantly for these heats, 10% for Heat P4 and 28% for Heat 64.

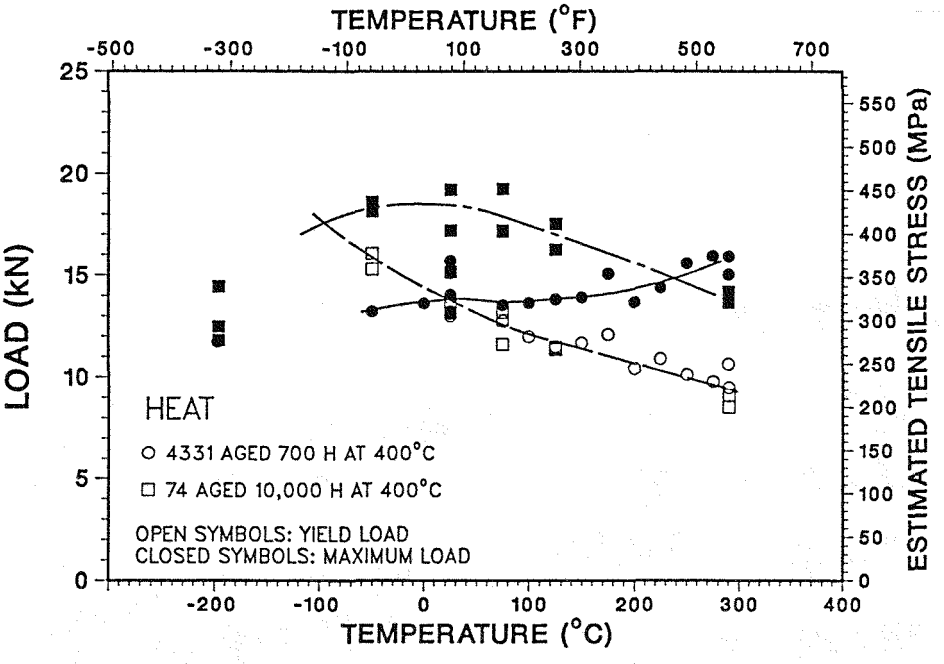

Figure 5. Yield and Maximum Loads from Charpy-Impact Data for Framatome Heat 4331 Aged for 700 h at 400°C and ANL Heat 74 Aged for 10,000 h at 400°C.

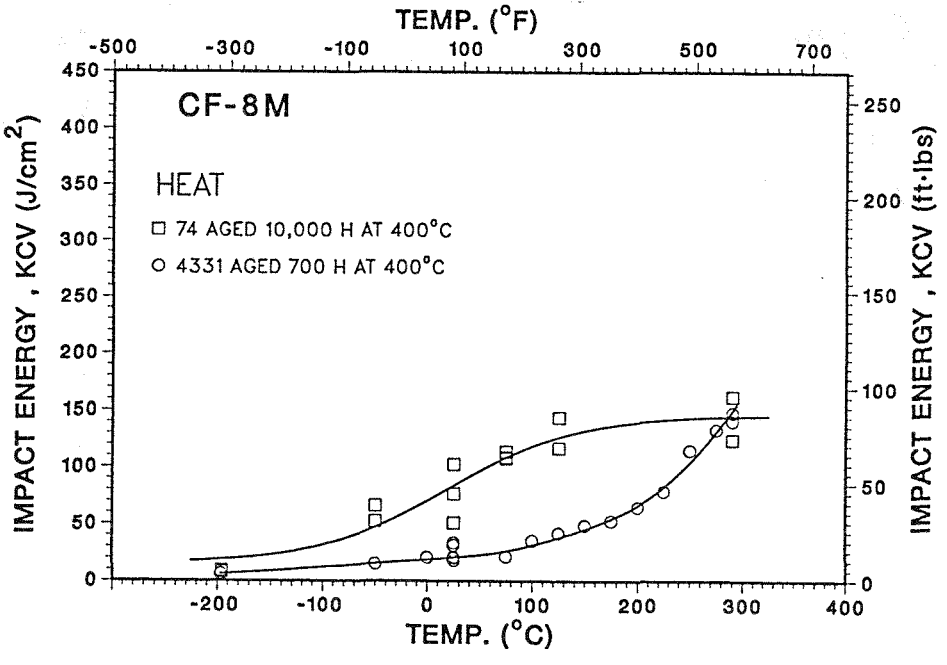

Figure 6. Charpy Transition Curves for Heats 4331 and 74 Aged at 400°C.

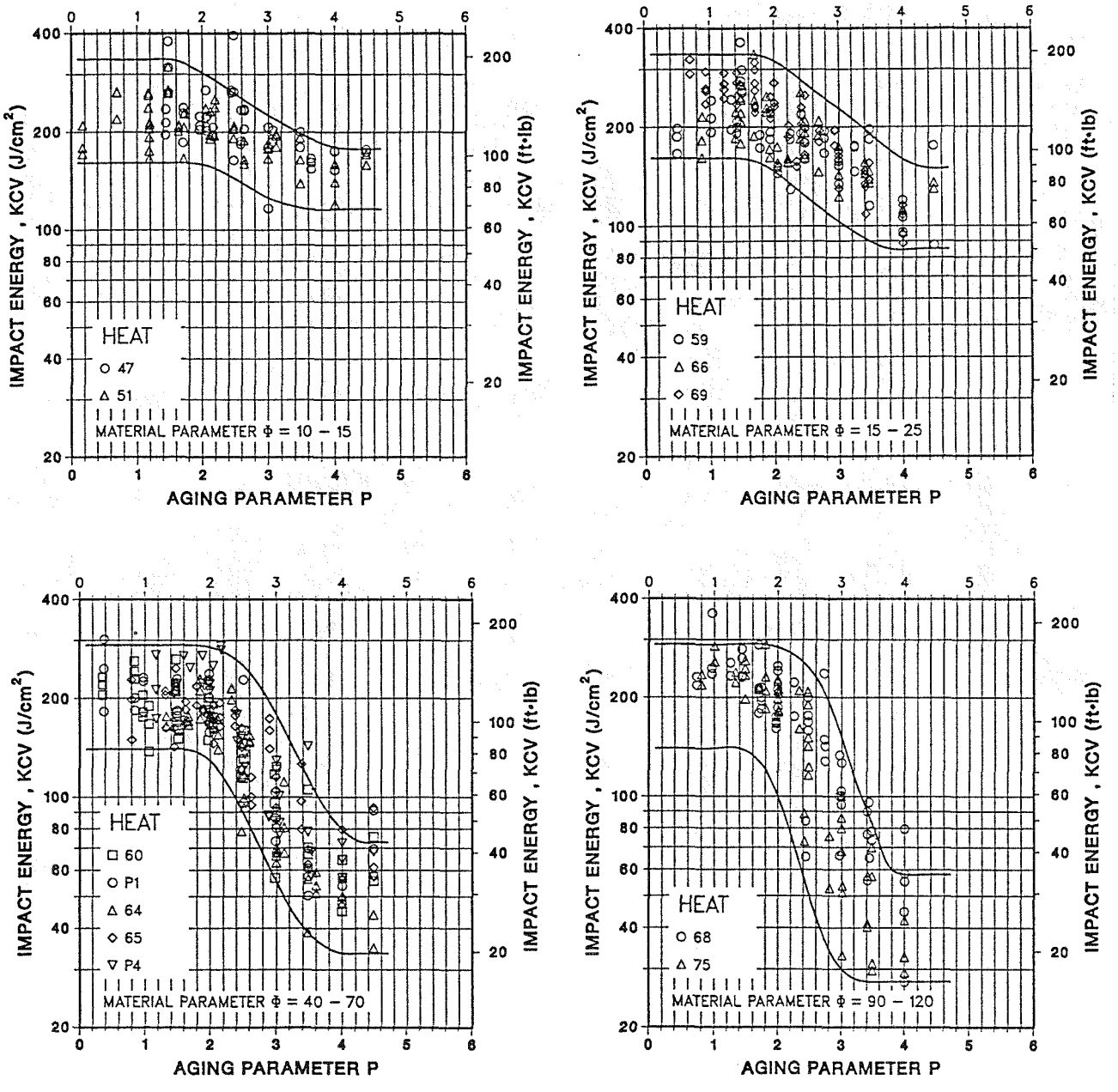

Figure 7. Effect of Thermal Aging on Room-Temperature Impact Energy of CF-3, CF-8, and CF-8M Steels with Different Range of Material Parameters Φ.

4. Charpy Transition Curves

Assessment of the extent of embrittlement at reactor operating temperatures requires an evaluation of aging effects on the Charpy transition curves. The Charpy data were fitted with a hyperbolic tangent function of the form

$$KCV = K_O + B\{1 + \tanh [(T-C)/D]\}, \quad (4)$$

where Ko is the lower-shelf energy, T is the test temperature, B is half the distance between upper- and lower-shelf energy, C is the mid-shelf Charpy transition temperature (CTT) in °C, and D is the half-width of the transition region. The best-fit curves for the three grades of cast stainless steel aged at 350°C for times up to 30,000 h are shown in Fig. 8. Thermal aging decreases the impact energy and shifts the transition curves to higher temperatures. The results suggest a "saturation effect" for upper-shelf energy (USE) after aging. The values of USE decrease significantly after aging for ~2600 h at 350°C and do not change for longer aging times. After saturation of USE, the decrease in impact energy is due to an increase in CTT, i.e., the value of B in Eq. (4) remains constant and only C and D increase with longer aging times. This behavior is observed at all aging temperatures and for all heats of material. The three heats have similar amounts of ferrite and the "saturation" values of USE are comparable. However, the shift in CTT is significantly different; the CF-8M steel exhibits the largest shift.

The room-temperature Charpy data, Fig. 7, indicate that for a specific range of material parameter Φ, a saturation value of minimum impact energy is reached when P is ~3.5, i.e., ~3,000 h at 400°C or ~30,000 h at 350°C. A similar saturation effect for the Charpy transition curves can not be established with any acceptable degree of confidence from the existing data. The transition curves for the three grades of cast stainless steel aged to P values between 3.4 and 4.0 are shown in Fig. 9. For Heat 69 (Φ ~14), the minimum room-temperature impact energy is close to USE. The transition curves for the three aging conditions are comparable and suggest a saturation effect, i.e., the curves represent the maximum CTT which would ever be achieved after long-term aging. A increase in CTT would mean a further decrease in room-temperature impact energy for Heat 69. The transition curves for Heat 68 (Φ~92) are also comparable but may not represent saturation condition. The minimum room-temperature impact energy is close to the lower-shelf energy; an increase in CTT would not significantly change the room-temperature impact energy.

Transition curves for Heat 75 (Φ~117) do not exhibit a saturation effect. The results indicate that although the room-temperature impact energy does not change for P values >3.5, the impact energy at reactor temperatures can continue to decrease with time. This behavior is not unique to CF-8M steels and has been observed in the EPRI study on CF-3 steel (Φ ~90).[14] Long-term aging data are needed to establish the impact energies at reactor temperatures and to determine whether a saturation effect in transition curves is achieved for some of the heats, e.g., heats with low values of material parameter Φ.

The transition curves for Heats 69, 68, and 75 also indicate that the transition curves for 350°C aging are lower than those after aging for equivalent time at 400°C, particularly for the CF-8M steel. The mid-shelf CTT for the three grades of cast stainless steel aged up to 30,000 h at 320, 350, and 400°C are plotted as a function of the aging parameter P in Fig. 10. For 350 or

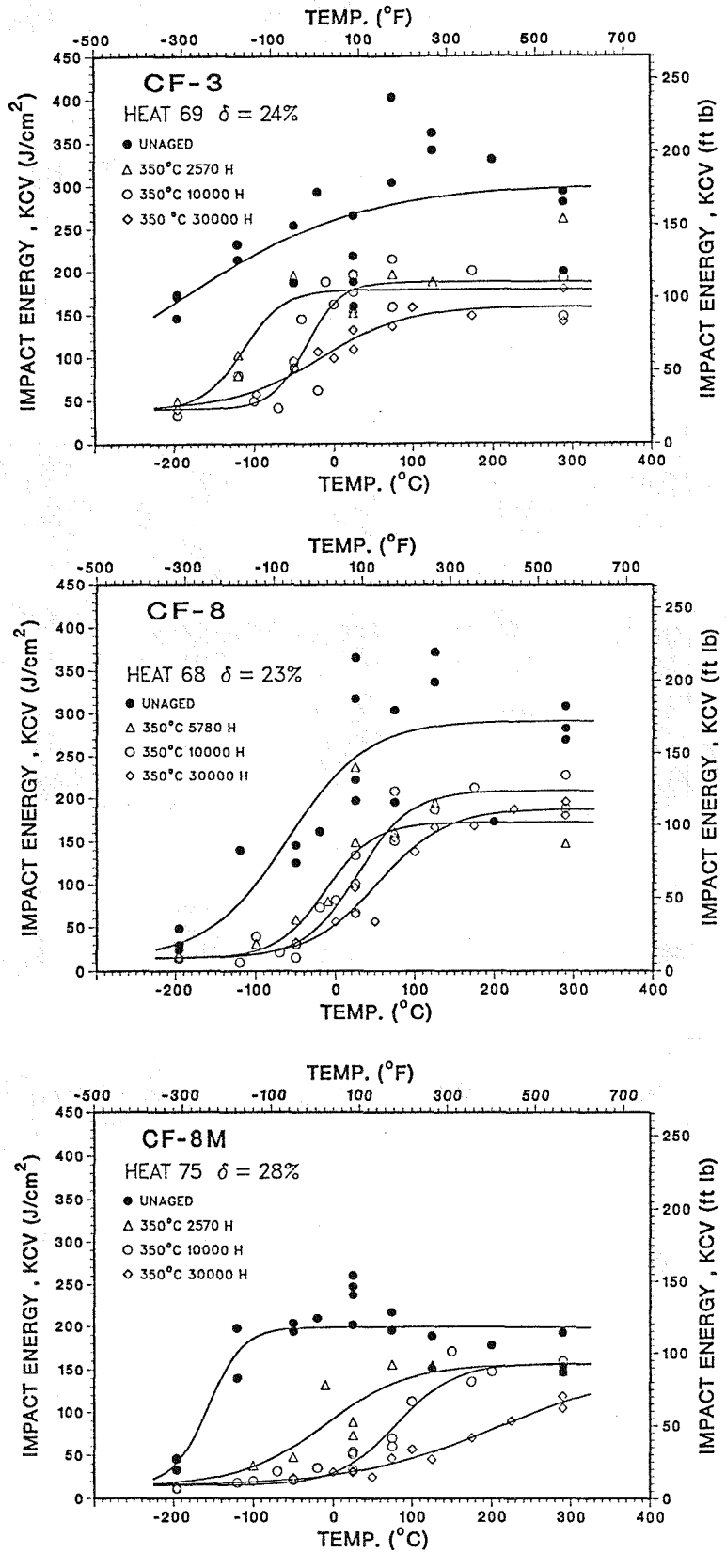

Figure 8. Effect of Aging Time on Charpy Transition Curves of CF-3, CF-8, and CF-8M Steels Aged at 350°C.

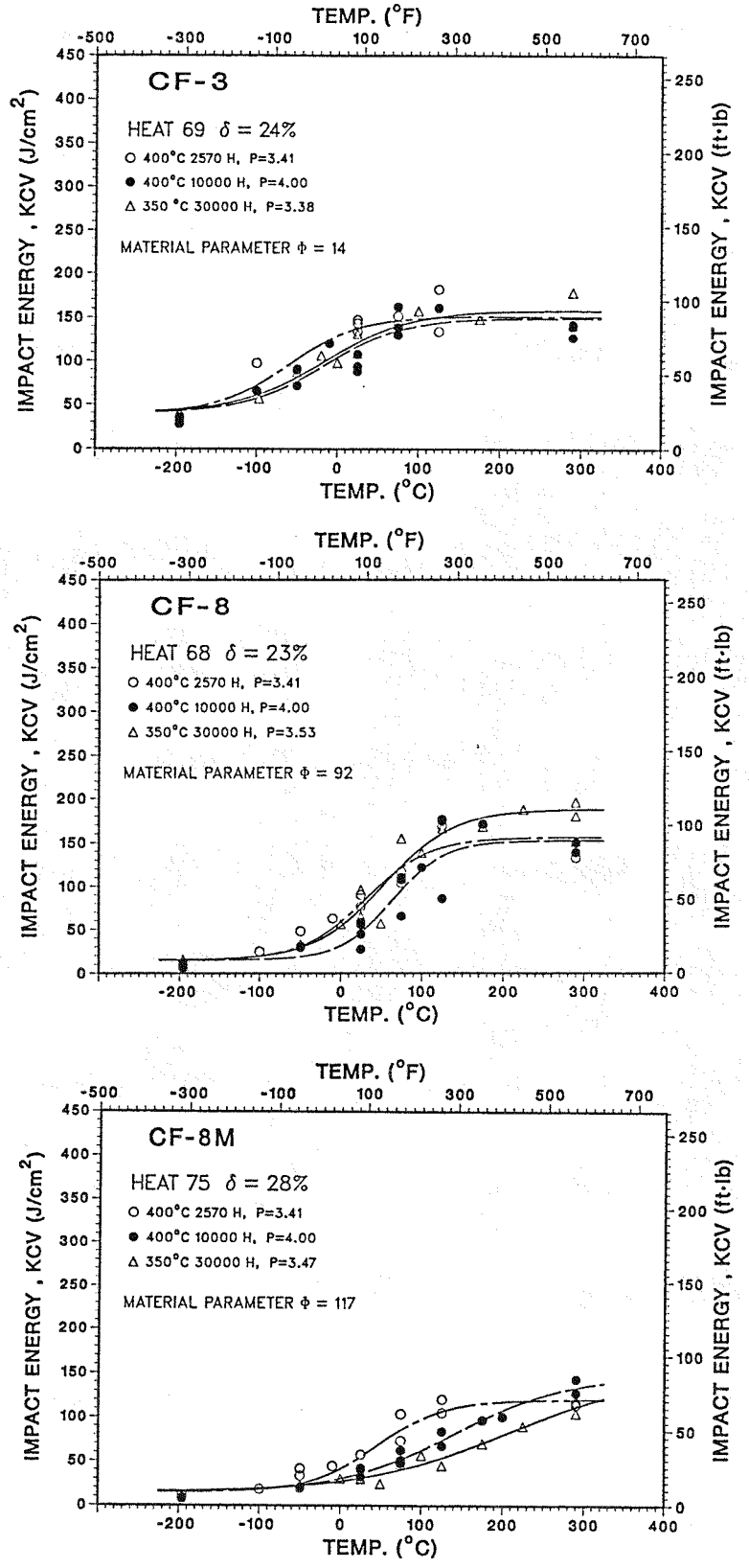

Figure 9. Charpy Transition Curves for CF-3, CF-8, and CF-8M Steels Aged to P Values between 3.4 and 4.0.

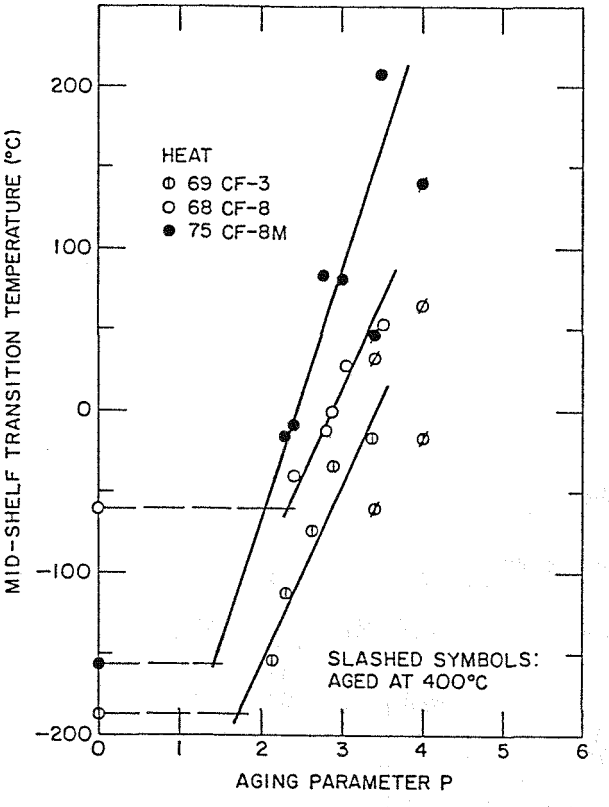

Figure 10. Change in Mid-Shelf Charpy Transition Temperature with Thermal Aging.

320°C aging, the change in CTT with P, i.e., slope of the lines in Fig. 10, is approximately the same for the three heats. However, the values of CTT for 400°C aging are lower than those after aging at 350°C.

These results raise an important issue, the kinetics of embrittlement established from the room-temperature Charpy data are not representative of the kinetics of embrittlement at reactor temperatures. The aging parameters P in Fig. 10 were calculated using the activation energies obtained from room-temperature data. These values of P may not be valid for the high-temperature results. The kinetics of embrittlement can not be obtained with any reasonable confidence from the high temperature data. The results often yield negative values of activation energy. Figures 8 and 9 show that the impact energy at 290°C decreases rapidly during the initial 3,000 h of aging and does not change significantly with longer aging times, particularly for heats with low values of Φ.

5. Fracture Toughness

The J-R tests were conducted at Materials Engineering Associates, Inc.,[15] and ANL on eight heats of cast stainless steel. The tests were performed on 1-T compact tension specimens according to ASTM specifications E813-85 and E1152. However, the values of J_{IC} were determined from the intersection of the power law curve with the 0.15-offset line rather than 0.2-offset line. J-R curve tests on cast stainless steels[12] indicate that a slope of 4 times the flow stress for the blunting line expresses the J *vs* Δa data better than the slope of 2 times the flow stress defined in E813-85. The values of J_{IC} reported in this paper were determined using a

slope of 2 times the flow stress for the blunting line. Consequently, the J_{IC} values would be slightly higher relative to the data from FRA study.[12] An average value of tearing modulus was determined from the power law curve between the exclusion lines. The results indicate that thermal aging decreases the fracture toughness J_{IC} and tearing modulus of the material at room temperature and at 290°C. The fracture toughness results are consistent with the Charpy-impact data, i.e., unaged and aged materials that show low impact strength also exhibit lower fracture toughness.

The fracture toughness J_{IC} values and Charpy V-notch impact energies obtained at room temperature are plotted in Fig. 11. Results from the studies at Westinghouse (WH),[16] FRA,[11,12] and EPRI[14] are also shown. For low values of toughness (i.e., J_{IC} <500 kJ/m^2), J_{IC} decreases linearly with impact energy. The dashed lines represent the lower-bound values. The slope of the lower-bound curve is 0.143 (dimensionless), which agrees well with the correlation between J and KCV proposed for flaw evaluation procedures for ferritic steel piping.[17] The tearing modulus also decreases with thermal aging. Figure 12 shows the room temperature values of tearing modulus and J_{IC} for various heats and aging conditions. The dashed lines represent the lower-bound values.

Figures 3, 11, and 12 can be used to estimate the minimum room-temperature fracture toughness of any specific cast stainless steel aged for long times. The minimum room-temperature impact energy is determined from Fig. 3 and the fracture toughness J_{IC} and tearing modulus are estimate from Figs. 11 and 12. For the various heats investigated, the maximum value of material parameter Φ was ~120. This would correspond to minimum room-temperature impact energy of ~30 J/cm^2 (~18 ft·lb) and J_{IC} and tearing modulus values of 40 kJ/m^2 and 30, respectively. The impact energy, J_{IC}, and tearing modulus of heats which are very sensitive to thermal aging (i.e., Φ >150) could be as low as 15 J/cm^2, 20 kJ/m^2, and 15, respectively.

The influence of thermal aging on fracture toughness at reactor temperatures is difficult to estimate accurately from the present data. As discussed in section 4, although the room-temperature impact energy reaches a minimum saturation value, the high temperature impact energy can continue to decrease. For some heats, the extent and kinetics of embrittlement determined from room-temperature data are not representative of embrittlement at reactor temperatures. Figure 13 shows a plot of J_{IC} values at 290°C as a function of room-temperature impact energies for various heats and aging conditions. The results indicate that the room-temperature lower bound curve, i.e., dashed line in Fig. 13, would yield a conservative estimate of J_{IC} at 290°C. Fracture toughness data from long-term aged material will be helpful in establishing the lower bound curve for J_{IC} at reactor temperature. The correlation between tearing modulus and J_{IC} values at 290°C is shown in Fig. 14.

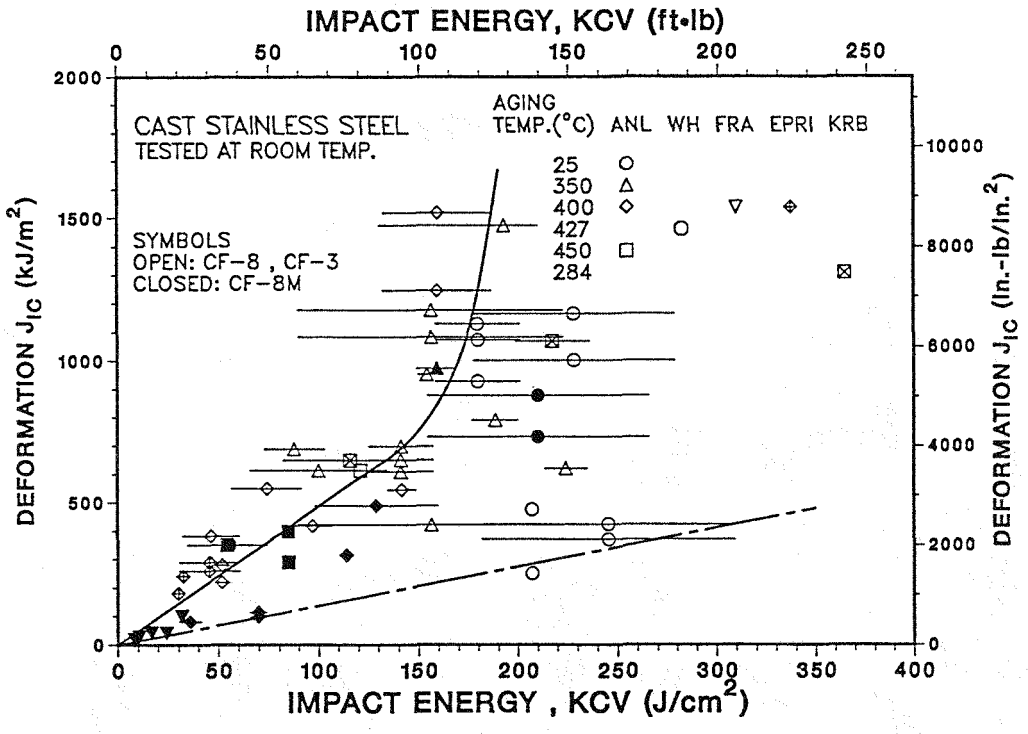

Figure 11. Correlation between Room Temperature Fracture Toughness J_{IC} and Impact Energy for Cast Stainless Steels

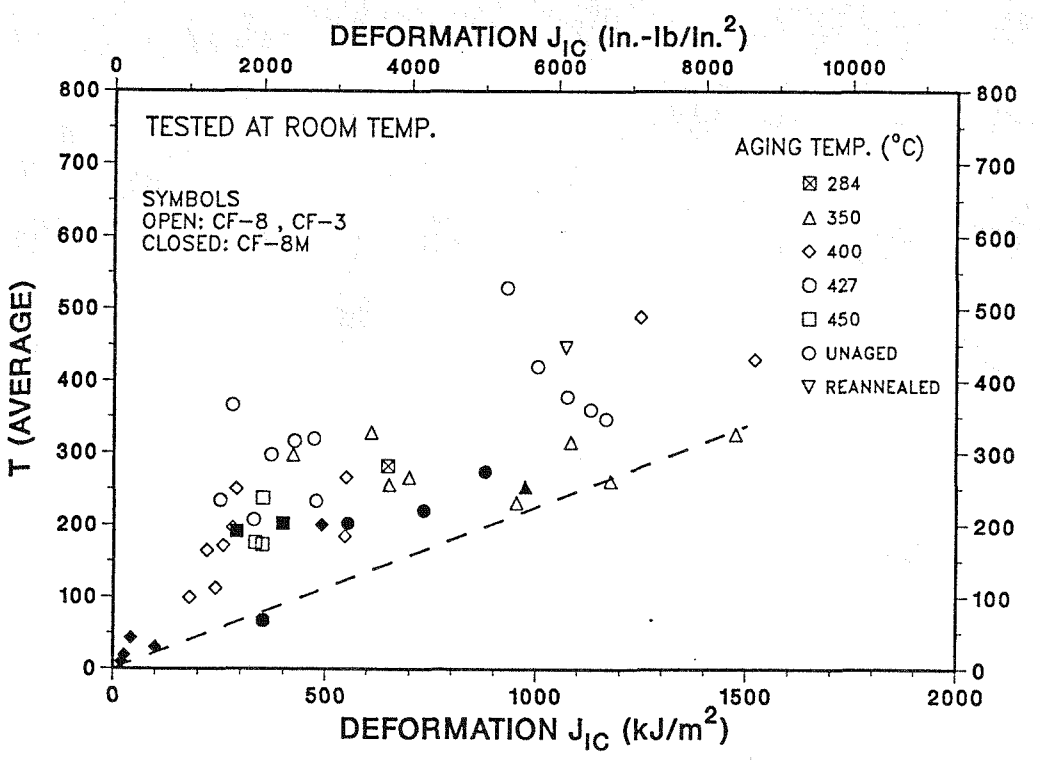

Figure 12. Correlation between Room Temperature Tearing Modulus (T) and Fracture Toughness J_{IC} Cast Stainless Steels.

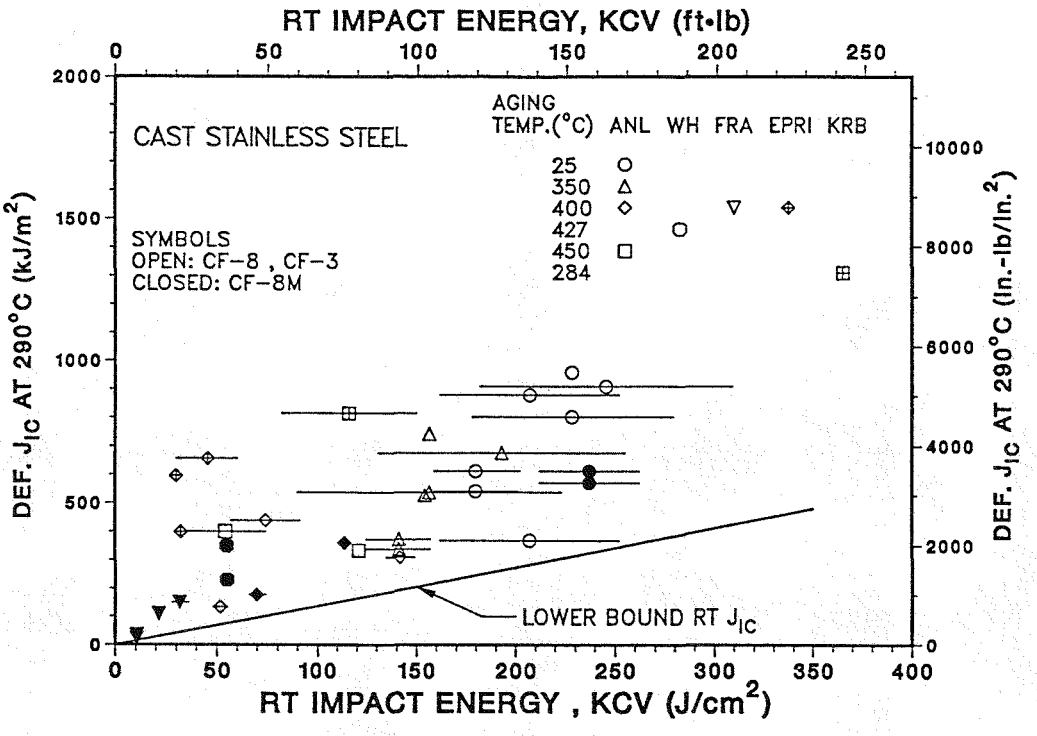

Figure 13. Correlation between Fracture Toughness J_{IC} and Room Temperature Impact Energy for Cast Stainless Steels.

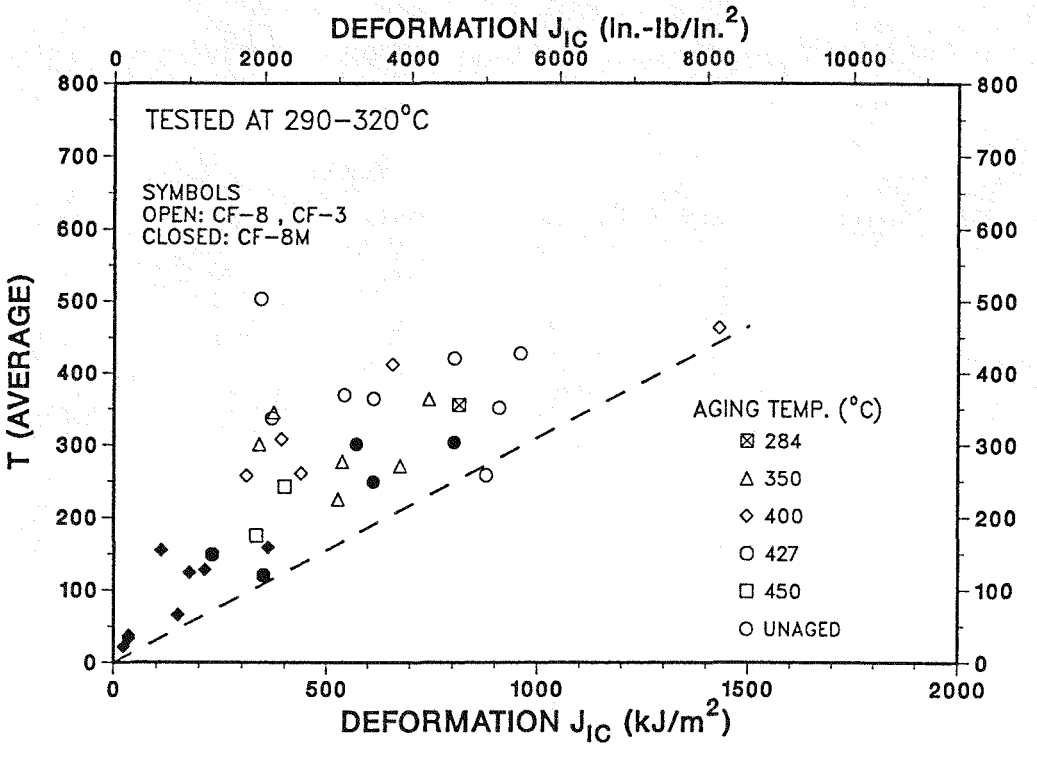

Figure 14. Correlation between the 290°C Tearing Modulus (T) and Fracture Toughness J_{IC} for Cast Stainless Steels.

6. Mechanisms of Embrittlement

Embrittlement of cast duplex stainless steel results in a brittle fracture associated with either cleavage of the ferrite phase or separation of the ferrite/austenite phase boundary. The degree of embrittlement is controlled by the amount of brittle fracture. Cast stainless steels with poor impact strength exhibit >80% brittle fracture. For some cast steels, although a fraction of the material may fail in a brittle fashion, the surrounding austenite provides the ductility and toughness. Such steels have adequate impact strength even after long-term aging. A predominantly brittle failure occurs when either the ferrite phase is continuous, e.g., in cast material with a large ferrite content, or the ferrite/austenite phase boundary provides an easy path for crack propagation, e.g., in high-carbon grades of cast steels with large phase-boundary carbides. Consequently, the amount, size, and distribution of the ferrite phase in the duplex structure and the presence of phase-boundary carbides are important parameters in controlling the degree or extent of embrittlement.

Thermal aging of cast stainless steels at temperatures of 300 to 450°C leads to the precipitation of additional phases in the ferrite matrix, e.g., formation of a Cr-rich α' phase by spinodal decomposition, nucleation and growth of α', precipitation of a Ni- and Si-rich G phase, γ_2 (austenite), and $M_{23}C_6$ carbide.[18-20] The additional phases provide the strengthening mechanism and strain hardening to increase the local tensile stress. Consequently, the critical stress level for brittle fracture is achieved at higher temperatures. Microstructural data indicate that the formation of α' by spinodal decomposition is the primary mechanism for strengthening.[8,18-20] Consequently, the kinetics of spinodal decomposition primarily control the overall rate of low-temperature embrittlement of cast stainless steel. Other precipitate phases have secondary effects on embrittlement.

Spinodal decomposition and G-phase precipitation in low-temperature aged cast stainless steel have been investigated by transmission electron microscopy (TEM), atom-probe field-ion microscopy (APFIM), small-angle neutron scattering (SANS), and extraction replica techniques.[18-24] The temperature dependence of the spinodal reaction in CF-3 stainless steel yields an activation energy of 250 ± 30 kJ/mole (59 ± 7 kcal/mole).[24] This value is comparable to that for Cr diffusion in Fe-Cr alloys and is significantly higher than the activation energy for low-temperature embrittlement obtained from mechanical property data [i.e., in the range of 65 to 230 kJ/mole (15 to 55 kcal/mole)]. The low values of activation energy for embrittlement are most likely due to the synergistic effects of other precipitate phases on embrittlement.

Precipitation of carbides or nitrides at the phase boundaries causes fracture by phase-boundary separation and facilitates cleavage of ferrite by particle cracking. Consequently, a lower degree of spinodal decomposition is needed for a given change in mechanical properties. Precipitation of carbides or nitrides occurs primarily at 450 or 400°C and is extremely slow at lower temperatures. The influence of phase-boundary carbides, thus, would tend to increase the apparent activation energy of embrittlement.

The other factor that can influence the overall kinetics of embrittlement is precipitation of the G phase, a multicomponent phase consisting of Ni, Si, Mo, Cr, Fe, and some Mn, and C.[21,22] Cast stainless steels which show precipitation of G phase after aging, generally exhibit faster kinetics of embrittlement. Also, the activation energy of embrittlement decreases with an increase in the volume fraction of G phase. The aging conditions in which G phase has been detected by TEM or SANS, in various aged cast stainless steels, are shown in Fig. 15. The kinetics for the decrease in the Charpy impact energy of aged cast stainless steel are also plotted in the figure. The solid lines represent the average time for 50 and 80% reduction in impact energy for the various ANL heats. Actual aging time for a given decrease in impact energy varied significantly for the various heats and is shown by the horizontal scatter bars. The aging times for the CF-8M steels were generally lower than those for the CF-3 or CF-8 steels. The results indicate that at 400°C, the reduction in impact energy is largely complete before G phase is detected in any of the heats. However, G-phase precipitation and the decrease in impact energy occur simultaneously at temperatures <350°C. These results suggest that the influence of G–phase precipitation on embrittlement would be greater at low temperatures. At 400°C, the kinetics of spinodal decomposition are much faster than G–phase precipitation, which follows nucleation and growth.

The exact nature of the effects of G phase on embrittlement are not well understood. A possible effect is the depletion of Ni and Mo from the ferrite matrix. The ferrite matrix typically contains ~5% Ni. The presence of Ni in single–phase Fe-Cr alloys is known to promote spinodal decomposition,[25] but alloys with >4% Ni take longer to embrittle than do

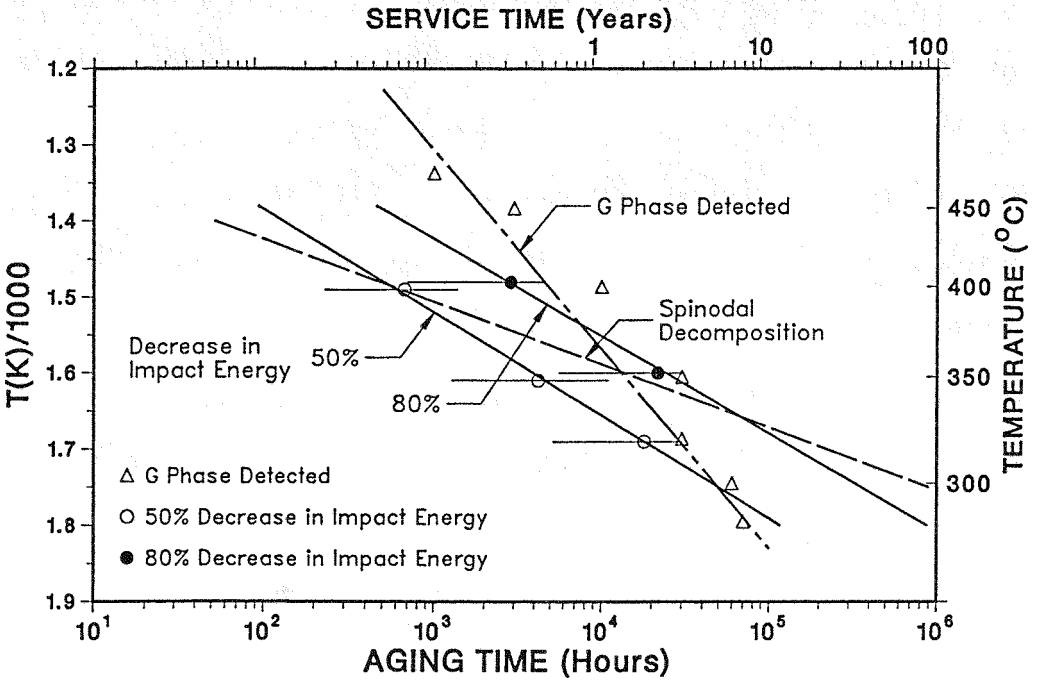

Figure 15. Arrhenius Plots for Precipitation of G Phase and Reduction in Charpy Impact Energy for Aged Cast Stainless Steels.

alloys with <4% Ni.[26] The aging times at 400 or 425°C required for 80% reduction in impact energy are a factor of ~3 slower for an Fe-26Cr-6Ni alloy than for the Fe-26Cr alloy.[26] Furthermore, at temperatures of 400 to 475°C, embrittlement of ferritic steels is faster than that of cast duplex stainless steels.[27] The seemingly opposite effects of Ni on spinodal decomposition and embrittlement in Fe-Cr alloys are attributed to promotion of twinning as a mode of deformation in alloys containing >4% Ni.[26,28-30] Addition of Mo to Fe-Cr alloys also promotes twinning.[28,30] Although spinodal decomposition is faster in Ni-containing alloys, it is less effective as a strengthening mechanism because of twinning as a mode of deformation. Consequently, a greater degree of spinodal decomposition would be needed for the same degree of embrittlement.

The precipitation of G phase can change the composition of ferrite , thus , alter the deformation behavior and fracture mode of aged cast stainless steels. Deformation twins in ferrite are observed in aged cast stainless steels at all test temperatures. Figure 16 shows twins in fractured Charpy Specimens of Heat P1 aged for 30,000 h at 350°C and tested at room temperature and 290°C. At high temperatures, the phase boundaries have a jagged appearance and have moved to accommodate the deformation due to twinning. Such adjustments in the phase boundaries are difficult at lower temperatures and cracks can form at twin/ phase boundary or twin/twin intersections. Twin boundary cracks are observed in aged cast steels. Heat P1 has a high activation energy, e.g., 239 kJ/mole (Table 2), and , thus, the contribution of G phase is expected to be negligible. The twinning behavior of heats with low activation energies is being investigated to establish the role of G phase on deformation and fracture mode of aged cast stainless steels.

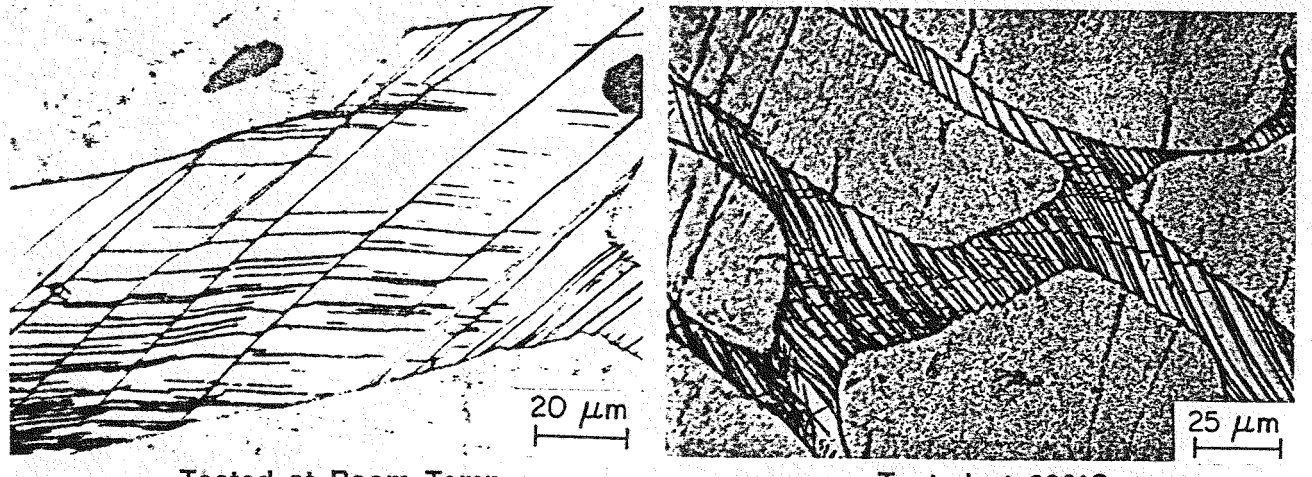

Figure 16. Deformation Twins in Charpy Impact Specimens of CF-8 Steel Aged for 30,000 h at 350°C and Tested at Room Temperature and 290°C.

7. Kinetics of Embrittlement

Results from the present study, together with data from FRA[11,12] and GF[1] studies, were analyzed to develop a correlation between the activation energy for embrittlement and the chemical composition, in wt.%, of the cast material. The results have been presented earlier.[9] The analyses yielded two separate correlations: one for the ANL and FRA data, given by

$$Q(kJ/mole) = 90.54 + 9.62\,Cr - 8.12\,Ni - 7.53\,Mo + 20.59\,Si - 123.0\,Mn + 317.7\,N \quad (5)$$

and the other for the GF data, given by

$$Q(kJ/mole) = -66.65 + 6.90\,Cr - 5.44\,Ni + 8.08\,Mo + 17.15\,Si + 44.1\,Mn + 297.1\,N \quad (6)$$

The activation energy values, reported in Ref. 9 were used in the analyses. The activation energies for Heats 68, 69, 75, and P4 were not included in the analyses. For these heats, the activation energies predicted from Eq. (5) are in good agreement with the experimental values, Table 2. Equation (5) also predicts accurately the kinetics of embrittlement observed in the CEGB study on three heats of CF-3 steel.[13]

The reasons why a unified expression could not be obtained for the two data sets and for the different effects of constituent elements in the two expressions are not clearly understood. As discussed in Section 6, the precipitation or growth of phase–boundary carbides or nitrides during aging would increase the activation energy for embrittlement. An increase in C or N in the steel will promote carbide or nitride precipitation and, thus, increase the activation energy. The positive sign of the coefficient for N agrees with this behavior; the correlation for the C content in the steel was poor.

The contribution of other elements, i.e., Ni, Si, Mo, and Mn, is expected on the basis of their effects on G-phase precipitation. These elements should promote G-phase precipitation and, hence, the coefficients for these elements should have a negative sign, since G–phase precipitation decreases the activation energy for embrittlement. The Si coefficient has a positive sign in both expressions, and the Mo and Mn coefficients are positive in Eq. (6). These results indicate that other factors, not included in the analysis, influence the kinetics of embrittlement. A possible factor may be the dislocation density in the ferrite matrix. The G phase precipitates preferentially at dislocations.[18-20] Consequently, the defect structure in the as-cast material will have a strong effect on G–phase precipitation. Mechanistic understanding of the variations in activation energy is desirable to avoid "surprises" in material composition. Information on the role of G phase on embrittlement could provide a unified correlation for all compositions.

8. Preliminary Assessment of Embrittlement

Embrittlement of any cast stainless steel component during reactor service can be estimated from the data obtained in the present study. Realistic estimates of impact strength and fracture toughness for a specific heat of cast stainless steel, as a function of time and temperature of reactor service, can be obtained in two steps. First, it is necessary to establish

the extent or degree of embrittlement, i.e., the minimum toughness that would ever be achieved for the material after long-term aging; then, the rate of decrease or the kinetics of embrittlement can be determined.

The material information required to estimate the degree of embrittlement is the chemical composition and the ferrite content and spacing. The minimum impact energy, K_m, is determined from the correlation between the material parameter Φ and impact energy, Fig. 3. Fracture toughness, i.e., J_{IC} and tearing modulus, is estimated from the correlations between J_{IC} and impact energy and between tearing modulus and J_{IC}, Figs. 11-14.

Figure 3 also indicates that the minimum room-temperature impact energy for the worst heat of cast stainless steel (i.e., a material parameter of >200) can be as low as 15 J/cm^2. This corresponds to a lower-bound J_{IC} of 20 kJ/m^2 and a tearing modulus of 15. The correlations for realistic estimates of fracture toughness at reactor temperatures have not yet been established. Available data indicate that the room temperature values are also applicable at reactor temperatures, however, the values may be too conservative for some compositions of cast stainless steels.

The rate of decrease of toughness, i.e., the kinetics of embrittlement, can be estimated from Eqs. (1), (2), and (5) when chemical composition and initial impact strength of the cast material are known. The constant β in Eq. (2) is obtained from the difference between the initial strength and minimum impact energy, K_m. The activation energy, Q, is determined from Eq. (5). The average value of the constant α in Eq. (2) is 1.0, and θ is 3.0 for CF-3 and CF-8 steels and 2.6 for CF-8M steel. The decrease in impact energy, as a function of time and temperature of reactor service, is determined from Eqs. (1) and (2).

Figure 17 shows examples of the predicted embrittlement behavior of heats susceptible to embrittlement (A and C) and typical heats of CF-8M and CF-8 cast stainless steel (B and D). The corresponding fracture toughness J_{IC} and tearing modulus can be determined from Figs. 11-14. Table 3 provides the theoretical chemical composition and the ferrite content and spacing of the heats. All compositions are within ASTM specification A351. The compositions of Heats A and C give high ferrite content and fast kinetics of embrittlement, i.e., low activation energy. The mean ferrite spacing for most cast stainless steels with >10% ferrite ranges from 40 to 200 μm; the average value for thick castings (e.g., GF heats or the KRB pump cover in Table 1) is ~175 μm. A large value of the ferrite spacing was selected for Heats A and C to obtain a conservative estimate of the extent of embrittlement.

The results show that the impact energies of Heats A and C will decrease to below 40 J/cm^2 after four or five years of service at 320°C. Heats B and D, with lower ferrite content (15%), exhibit much less embrittlement, i.e., the impact energy will not decrease below 90 J/cm^2 even after long service. The kinetics of embrittlement are also slower for these heats. The results also show that the minimum impact energy is important in estimating the embrittlement behavior. Slow kinetics of embrittlement, i.e., a high activation energy, delay the decrease in impact strength, but the material would reach the lowest value of impact strength after long reactor service. This behavior is seen for Heat E, which has the same

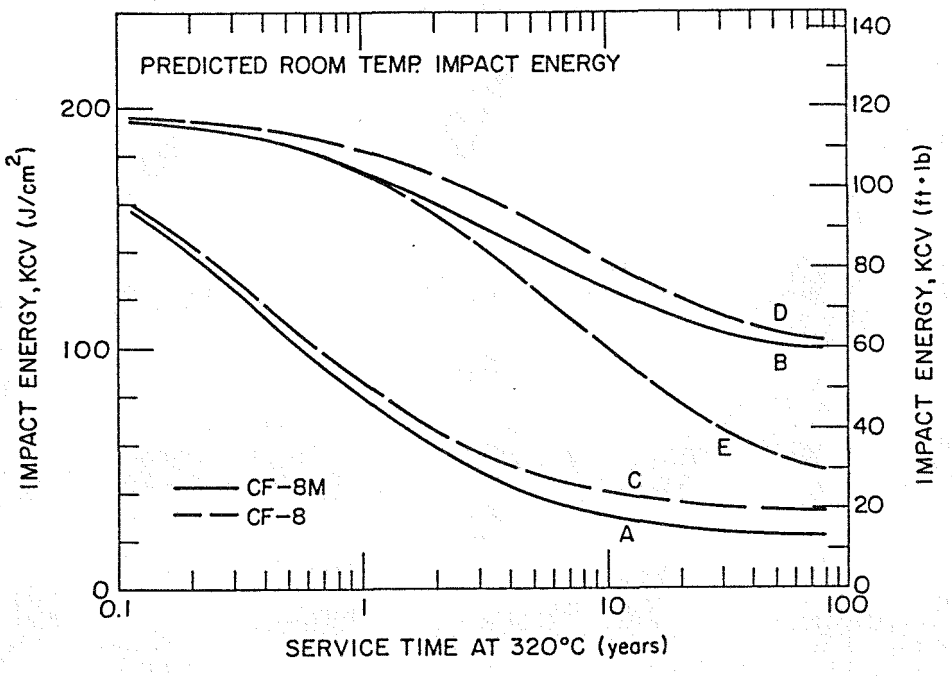

Figure 17. Predicted Embrittlement Behavior of CF-8M and CF-8 Cast Stainless Steel.

Table 3. Theoretical Chemical Composition and Ferrite Morphology of Cast Stainless Steel used for Predicting Embrittlement under LWR Conditions

		Composition (wt %)							Ferrite			
									Cont.[a]	Spacing[b]	Q^c	K_m^d
Heat	Grade	C	N	Mn	Si	Ni	Cr	Mo	(%)	(μm)	(kJ/mole)	(J/cm^2)
A	CF-8M	0.05	0.02	1.2	1.2	10.0	21.0	2.6	28	180	75	20
B	CF-8M	0.05	0.05	0.5	1.0	9.0	19.5	2.0	15	80	167	90
C	CF-8	0.04	0.02	1.3	0.5	8.4	21.0	0.4	24	200	75	30
D	CF-8	0.05	0.05	0.5	1.0	8.5	20.5	0.4	15	80	188	90
E	CF-8	0.04	0.02	1.3	0.5	8.4	21.0	0.4	24	200	188	30

[a]Calculated from chemical composition with Hull's equivalent factor.

[b]Assumed values.

[c]Calculated from Eq. (5), value for heat E was arbitrarily assumed.

[d]Determined from Fig. 3.

material parameters as Heat C, but the activation energy was arbitrarily assumed to be 188 kJ/mole, rather than the calculated value of 75 kJ/mole, to illustrate the effect of slower kinetics. Even with very slow kinetics, impact energy decreases to ~40 J/cm^2 after ~40 yr of service.

9. Conclusions

Charpy-impact and J-R curve data for several experimental and commercial heats of cast stainless steel are presented. The materials were thermally aged up to 30,000 h at temperatures of 290 to 450°C. The results indicate that aging at these temperatures leads to an increase in tensile strength and a decrease in impact energy, fracture toughness (J_{IC}), and tearing modulus of the material. The Charpy transition curve shifts to higher temperatures. The J_{IC} values are consistent with the Charpy-impact data, i.e., the relative reduction in impact energy is similar to the relative decrease in J_{IC} values. In general, the low carbon CF-3 grades of cast stainless steels are the most resistant, and while Mo-containing high-carbon CF-8M grades are the most susceptible to low-temperature embrittlement.

The effects of material variables on the embrittlement of cast stainless steels have been evaluated. The chemical composition of the steel and the ferrite content and spacing are important parameters in controlling the extent and kinetics of embrittlement. Ferrite morphology has a strong effect on the extent of embrittlement, while material composition influences the kinetics of embrittlement. Small changes in the constituent elements of the cast material can cause the kinetics of embrittlement to vary significantly.

The mechanisms of embrittlement of cast duplex stainless steel have been discussed. Embrittlement is caused by brittle fracture associated with either cleavage of ferrite or separation of ferrite/austenite phase boundaries. The formation of the α' phase by spinodal decomposition of the ferrite provides the strengthening mechanism to raise the local tensile stress above the critical value for cleavage and thus promotes brittle fracture. Precipitation and/or growth of phase–boundary carbides or nitrides leads to brittle failure by phase–boundary separation and also facilitates cleavage of the ferrite by particle cracking. Therefore, the degree of brittle fracture and, hence, the degree of embrittlement of a specific heat of cast stainless steel depends strongly on the amount and spacing of the ferrite in the duplex structure.

The kinetics of embrittlement are controlled by spinodal decomposition, precipitation and growth of phase boundary carbides, and precipitation of the G phase in ferrite. The rate of embrittlement for a specific cast stainless steel depends on the relative contributions of carbide and G-phase precipitation; activation energies can range from 65 to 230 kJ/mole.

Mechanical–property results from the present study and data from other investigations have been analyzed to develop the procedure and correlations for predicting the kinetics and extent of embrittlement of reactor components from known material parameters. The method and examples of estimating the impact strength and fracture toughness of cast components during reactor service are described. Results indicate that the lower–bound values of impact

energy, fracture toughness J_{IC}, and tearing modulus at room temperature could be as low as 15 J/cm^2, 20 kJ/m^2, and 15, respectively. Available data indicate that the lower-bound values at room-temperature may also be applicable at reactor temperatures. These values are probably very conservative for most materials. The range of material parameters representative of reactor components should be defined for realistic estimates of the lower–bound fracture toughness of cast components.

Acknowledgements

This work was supported by the Office of the Nuclear Regulatory Research in the U. S. Nuclear Regulatory Commission. The authors are grateful to A. Sather, W. K. Soppet, G. M. Dragel, and L. Bush for experimental contributions. The authors also wish to thank J. Muscara, W. J. Shack, and T. F. Kassner for their helpful discussions.

References

1. A. Trautwein and W. Gysel, "Influence of Long Time Aging of CF–8 and CF–8M Cast Steel at Temperatures Between 300 and 500°C on the Impact Toughness and the Structure Properties", *Stainless Steel Castings*, ed. V. G. Behal and A. S. Melilli, ASTM STP 756, Philadelphia, p. 165 (1982).

2. O. K. Chopra and H. M. Chung, *Long-Term Embrittlement of Cast Duplex Stainless Steels in LWR Systems: Annual Report, October 1983-September 1984*, NUREG/CR-4204, ANL-85-20 (March 1985); Nucl. Eng. Des., 89, 305 (1985).

3. O. K. Chopra and H. M. Chung, *Long-Term Embrittlement of Cast Duplex Stainless Steels in LWR Systems: Annual Report, October 1984-September 1985*, NUREG/CR-4503, ANL-86-3 (January 1986).

4. O. K. Chopra and H. M. Chung, *Long-Term Embrittlement of Cast Duplex Stainless Steels in LWR Systems: Semiannual Report, October 1985-March 1986*, NUREG/CR-4744 Vol. I, No. 1, ANL-86-54 (September 1986).

5. O. K. Chopra and G. Ayrault, in *Materials Science and Technology Division Light-Water-Reactor Safety Research Program: Quarterly Progress Report*, October-December 1983, NUREG/CR-3689 Vol. IV, ANL-83-85 Vol. IV, p. 129 (August 1984).

6. O. K. Chopra and H. M. Chung, in *Materials Science and Technology Division Light-Water-Reactor Safety Materials Engineering Research Programs: Quarterly Progress Report*, January-March 1984, NUREG/CR-3998 Vol. I, ANL-84-60 Vol. I, p. 52 (September 1984).

7. O. K. Chopra and H. M. Chung, "Aging Degradation of Cast Stainless Steels: Effects on Mechanical Properties," in *Environmental Degradation of Materials in Nuclear Power Systems-Water Reactors*, G. J. Theus and J. R. Weeks, eds., The Metallurgical Society, Warrendale, p. 737 (1988).

8. O. K. Chopra and H. M. Chung, "Effect of Low-Temperature Aging on the Mechanical Properties of Cast Stainless Steels," in *Properties of Stainless Steels in Elevated Temperature Service*, M. Prager, ed., MPC-Vol. 26/PVP-Vol. 132, ASME, New York, p. 79 (1988).

9. O. K. Chopra and H. M. Chung, "Initial Assessment of the Processes and Significance of Thermal Aging in Cast Stainless Steels," in *Proc. 16th Water Reactor Safety Information Meeting*, U. S. Nuclear Regulatory Commission, NUREG/CP-0097 Vol.3, p. 519 (March 1989).

10. S. Bonnet, J. Bourgoin, J. Champredonde, D. Guttmann, and M. Guttmann, "Evolution of Mechanical Properties of Various Cast Duplex Stainless Steels in Relation to Metallurgical and Aging Parameters: An Outline of Current EDF Programmes," presented at *Intnl. Workshop: Intermediate Temperature Embrittlement Processes in Duplex Stainless Steels*, August 1-2, 1989, Oxford, UK.

11. G. Slama, P. Petrequin, and T. Magep, "Effect of Aging on Mechanical Properties of Austenitic Stainless Steel Castings and Welds," presented at *SMIRT Post-Conference Seminar 6, Assuring Structural Integrity of Steel Reactor Pressure Boundary Components*, August 29–30, 1983, Monterey, CA.

12. Y. Meyzaud, P. Ould, P. Balladon, M. Bethmont, and P. Soulat, "Tearing Resistance of Aged Cast Austenitic Stainless Steel," presented at *Intl. Conf. on Thermal Reactor Safety (NUCSAFE 88)*, October 1988, Avignon, France.

13. P. H. Pumphrey and K. N. Akhurst, "The Aging Kinetics of CF-3 Cast Stainless Steel in the Temperature Range 300°C to 400°C," presented at *Intnl. Workshop: Intermediate Temperature Embrittlement Processes in Duplex Stainless Steels*, August 1-2, 1989, Oxford, UK.

14. P. McConnell and J. W. Sheckherd, Fracture Toughness Characterization of Thermally Embrittled Cast Duplex Stainless Steel, Electric Power Research Institute Report NP-5439 (September 1987).

15. A. L. Hiser, Tensile and J–R Curve Characterization of Thermally Aged Cast Stainless Steels, Materials Engineering Associates, Inc., NUREG/CR–5024, MEA–2229 (September 1988).

16. E. I. Landerman and W. H. Bamford, "Fracture Toughness and Fatigue Characteristics of Centrifugally Cast Type 316 Stainless Steel Pipe after Simulated Thermal Service Conditions," in *Ductility and Toughness Considerations in Elevated Temperature Service*, ASME MPC–8, p. 99 (1978).

17. A. Zahoor, R. M. Gamble, H. S. Mehta, S. Yukawa, and S. Ranganath, Evaluation of Flaws in Carbon Steel Piping, Electric Power Research Institute Report NP-4824M (October 1986).

18. H. M. Chung and O. K. Chopra, "Microstructure of Cast Duplex Stainless Steel after Long-Term Aging," in *Proc. Second Intl. Symp. on Environmental Degradation of Materials in Nuclear Power Systems - Water Reactors*, American Nuclear Society, LaGrange Park, IL, p. 287 (1986).

19. H. M. Chung and O. K. Chopra, "Kinetics and Mechanism of Thermal Aging Embrittlement of Duplex Stainless Steels," in *Environmental Degradation of Materials in Nuclear Power Systems - Water Reactors*, ed. G. J. Theus and J. R. Weeks, The Metallurgical Society, Warrendale, PA, p. 359 (1988).

20. H. M. Chung and O. K. Chopra, "Long-Term-Aging Embrittlement of Cast Austenitic Stainless Steels - Mechanism and Kinetics," in *Properties of Stainless Steels in Elevated Temperature Service*, ed. M. Prager, MPC-Vol. 26/PVP-Vol. 132, ASME, New York, p. 17 (1988).

21. J. Bentley, M. K. Miller, S. S. Brenner, and J. A. Spitznagel, "Identification of G-Phase in Aged Cast CF-8 Type Stainless Steel," in *Proc. 43rd. Electron Microscopy Society of America*, ed. G. W. Bailey, San Francisco Press, p. 328 (1985).

22. M. Vrinat, R. Cozar, and Y. Meyzaud, "Precipitated Phases in the Ferrite of Aged Cast Duplex Stainless Steel," *Scripta Met.* **20**, p. 1101 (1986).

23. T. J. Godfrey and G. D. W. Smith, "The Atom Probe Analysis of a Cast Duplex Stainless Steel," *J. de Physique*, Colloque C7, Vol. 47, suppl. to No. 11, p. 217(1986).

24. J. M. Sassen et al., "Kinetics of Spinodal Reaction in the Ferrite Phase of a Duplex Stainless Steel," in *Properties of Stainless Steels in Elevated Temperature Service*, ed. M. Prager, MPC-Vol. 26/PVP-Vol. 132, ASME, New York, p. 65 (1988).

25. H. D. Solomon and L. M. Levinson, "Mössbauer Effect Study of 475°C Embrittlement of Duplex and Ferritic Stainless Steels," *Acta Met.* **26**, p. 429 (1978).

26. K. Nakano, M. Kanao, and A. Hoshino, "Effect of Nickel Content and the Austenite Phase on Low Temperature Toughness and Embrittlement Behavior of Fe-26%Cr Alloys," *Trans. National Research Inst. for Metals* **20** , p. 1 (1978).

27. P. J. Grobner, "The 885°F (475°C) Embrittlement of Ferritic Stainless Steels," *Metal. Trans.* **4**, p. 251 (1973).

28. T. Magnin and F. Moret, "Mechanical Twinning in Ferritic Stainless Steels," *Scripta Met.* **16**, p. 1225 (1982).

29. T. Magnin, J. LeCoze, and A. Desestret, "Twinning and Stress Corrosion Cracking of Ferritic Phase of Duplex Stainless Steels," in *Duplex Stainless Steels*, R. A. Lula, ed., American Society for Metals, Metals Park, Ohio, p. 535 (1983).

30. M. Anglada. M. Nasarre, and J. A. Planell, "High Temperature Mechanical Twinning of Two Fe–Cr–Mo–Ni Ferritic Stainless Steels," *Scripta Met.* **21**, p. 931 (1987).